ORIGINAL ARTICLE

Acid resistance enhancement of human tooth enamel surface by Nd:YAG laser and incorporating silver nanoparticles: in vitro study

Walid K. Hamoudi[1] · Raid A. Ismail[1] · Zinah S. Shakir[1] · Amera Alkaisi[2]

Abstract

Purpose This work was devoted to assess the use of Nd:YAG laser with and without nanosilver particles to enhance tooth resistance of dental enamel against carries.
Method Forty-eight tooth samples were randomly divided into three main groups and received different treatments. Samples of group 1 were illuminated by a single pulse at different laser fluences, while those of group 2 received different number of laser pulses at fixed laser fluence, and finally the samples of group 3 received laser and colloidal silver nanoparticle treatments at different conditions. The samples were subjected to Vickers microhardness test, atomic force microscopy analysis, scanning electron microscopy observation, energy dispersive spectroscopy investigation, and demineralization and re-mineralization tests.
Results Due to fast laser heating and quenching, a significant microhardness increase in the treated dental enamel samples was seen. This resulted in an improvement in the enamel resistance against acids because of the decrease in hydroxyapatite lattice stress and the reduction in enamel solubility. The addition of silver nanoparticles to the laser-treated enamel surface helped stabilize the granules of the enamel surface tissue under the effect of laser irradiation. The demineralization of laser-treated samples showed higher Ca/P ratios than control group, indicating a higher resistance against acids.
Conclusion The combined laser illumination and the addition of silver nanoparticles lowered the tooth abrasion degree and increased tooth resistance to decay. The demineralized samples of all laser-treated samples had higher Ca/P ratios compared to the demineralized control sample. Laser energy has modified the Ca/P mineral ratio and forms steadier and lesser acid soluble compositions.

Keywords Dental enamel · Nd:YAG laser · Silver nanoparticles · Demineralization rate · Tooth decay reduction

Introduction

Dental decay is a very common disease during childhood and adolescence. Acids are generated by cariogenic bacteria in dental plaque spread inside the dental hard tissue during carbohydrate metabolism, causing mineral component dissolution [1, 2]. Although fluoride is used to prevent tooth decay, however, to control dental caries completely, a new method is still necessary (Florin et al., 1990). Since the 1960s, the efficiency of lasers for increasing the acid

resistance of enamel has been confirmed; moreover, when combined with fluoride, the effect will be further increased in the reduction of enamel solubility which increases the acid resistance of the enamel (Stern and Soggnaes, 1972; Marquez et al. 1993; Attin et al., 1997 [3–6]. Stern and Soggnaes (1972) [7] were the first to demonstrate that tooth acid resistance increases when irradiating the enamel surface by laser [8]. They reported that irradiating the tooth by laser can decrease its demineralization by 15% compared to untreated tooth. Wen et al. used pulsed Nd:YAG laser to increase the tensile bond strength (TBS) of resin and caries resistance of human enamel. Pre-treatment of enamel surface with Pulsed Nd:YAG laser method presents a potential clinical application, especially for the caries-susceptible population or individuals with recently bleached teeth. A dental tissue irradiated by laser light at suitable energy and time results in melting and re-crystallization and leads to some chemical and morphological changes in the structure

✉ Walid K. Hamoudi
  wjuaini2007@yahoo.com

1 Department of Applied Sciences, University of Technology, Baghdad, Iraq

2 Department of Dentistry, Al-Farabi University College, Baghdad, Iraq

Fig. 1 The procedural chart of the study
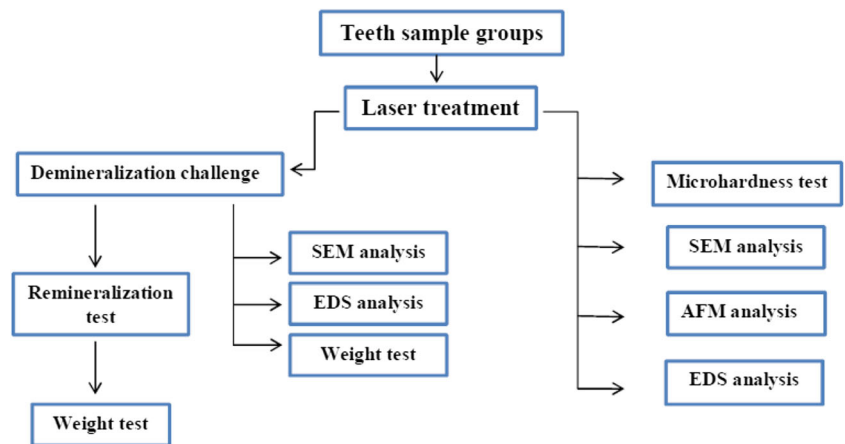
[9]. This process is associated with changes in dental hard tissue phases where mineral phases transform into a less soluble primary hydroxyapatite phase [10]. The actual laser role is materialized by its heating effect which raises the temperature of the dental tissue to a very high value at the irradiated spot. Consequently, the dental tissues melt and vaporize at the irradiation site, and a crater is created on the surface [11]. Nanosecond laser pulses are preferred in dental hard tissues treatment because of the short thermal diffusion time which will only go on within the laser pulse duration [12]. This minimizes the thermal damage, and therefore, sufficient energy can be confined and delivered at a local spot using multiple laser pulses. Some studies suggested combining Nd:YAG laser with topical fluoride to prevent dental caries. This combination was aimed to decrease acid demineralization of enamel in permanent teeth. Besides; it aimed at reducing dental caries in pit and fissure areas and on the smooth surfaces of the teeth (Tagomori and Morioka, 1989 [13]; Huang et al., 2001) [14]. Despite that, a group of researchers concluded no effective results from this combination (Azevedo et al., 2012) [15]. Another research group reported that pulsed Nd:YAG laser combined with casein-phosphor-peptide-amorphous calcium phosphate and fluoride decreases dental enamel demineralization (Abdulahhab & Mahmood, 2015) [16]. Neodymium laser, operating at 1064 nm wavelength, is weakly absorbed by hydroxyapatite elements of the enamel, and without a photo-sensitizer, an amount of laser energy would be transmitted to the pulp and risks its vitality [17]. New method to diminish caries rates is required to increase dental protection. Silver nanoparticle is safe when applied in human, eco-friendly, with outstanding antimicrobial properties against the growth of dental decay pathogens (*Mutans streptococci* and *Lactobacilli*), low in cost, and has longtime stability (3 years) [18, 19]. The aim of this work is to assess the effect of Nd:YAG laser and silver nanoparticles on the enhancement of tooth resistance against caries.

Material and methods

Fourty-eigth mature molars and premolars freshly extracted teeth samples in good dental health with no active decay or other diseases were stored in 10% formalin. The teeth were put in plastic molds; then, epoxy resin was mixed with small amount of epoxy hardener and slightly warmed up, to help solidify rapidly, and then poured on the teeth in the molds with the polished surfaces exposed. These molds were lifted after the epoxy became hard. The teeth were then sectioned either longitudinally or transversely into two samples using a low-speed diamond wheel saw (MTI Corporation, model SYJ-150) under water cooling. The samples were polished, under water spray cooling, using grinding machine (grinder polisher MPD 200-Dual Speed Polisher, Laree Technology CO. LTD, China) at speeds between 150 and 300 r/min and Amery silicon carbide papers from no. 1200 to 3000. At the final polishing stage, a cloth and 0.05 polishing alumina were utilized in metallurgical polisher (DP-U4, Struers-Denmark), at a low speed, with a light load on the samples. The samples were then cleaned ultrasonically by using Lab Tech, Daihan Labtech Co., LTD, model LUC-410, Korea, in distilled water for 5 min and stored in distilled water at room temperature. Q-switched Nd:YAG laser, supplied by HUAFEL, Single Pulse Mode, China, operating at 1064 nm wavelength, and providing up to 1 J 9 ns laser pulses, was employed to irradiate the teeth enamel surfaces. A positive lens of 10 cm focal length
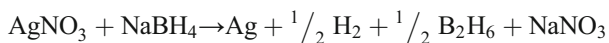
Table 1 Laser treatments of the tooth sample subgroups of group 1

Subgroup	Energy (J)	Number of pulses	Laser fluence (J/cm^2)
A	Control	0	0
B	300 mJ	1	38.2
C	400 mJ	1	50.95
D	500 mJ	1	63.69
E	600 mJ	1	76.43
F	700 mJ	1	89.17

Table 2 Laser treatments of the tooth sample subgroups of group 2

Subgroup	Energy (J)	Number of pulses	Laser fluence (J/cm^2)
A	Control	0	0
G	100 mJ	2	25.477
H	100 mJ	3	38.2
I	100 mJ	4	50.95
J	100 mJ	5	63.69
K	100 mJ	6	76.43

Table 4 Vickers microhardness test results for group 1

Subgroup name	Laser energy	No. of pulses	Microhardness (VHN)
A	0	0	403 ± 55
B	300	1	552.467 ± 73
C	400	1	590 ± 16
D	500	1	632.867 ± 89
E	600	1	639.4 ± 72
F	700	1	575.2 ± 97

was used to obtain the required laser energy fluence on the enamel surface, with laser spot diameter of 0.8 mm. Silver nanoparticles were prepared chemically by reducing silver nitrate ($AgNO_3$) using sodium boro-hydride ($NaBH_4$). Four-milliliter 0.001 M ($AgNO_3$) was added at a rate of one drop per second to 60 mL 0.002 M ($NaBH_4$) and the mixture was placed in an ice bath (to slow the reaction) and stirred by a magnetic stirrer for about 30 min. A light yellow transparent solution was formed as silver nanocolloidal by the reduction of silver ions as in the following equation:

$$AgNO_3 + NaBH_4 \rightarrow Ag + {}^1\!/_2\, H_2 + {}^1\!/_2\, B_2H_6 + NaNO_3$$

An atomic force microscope (SPM-AA3000, AFM-Contact mode, Angstrom Advanced Inc., USA) was employed to evaluate the surface roughness changes of the tooth enamel, before and after laser treatments. Two samples from each group were gold-coated for scanning electron microscope analysis using (Tescan, vega3, Czech) SEM microscope to recognize structural changes of the enamel surfaces after each treatment. Laser-treated and control samples were tested by energy dispersive X-ray spectrometer (EDS) (Angstrom Advanced, AIS2300 Multi-function SEM System, USA) to evaluate the changes in the elements' weight percentage of the enamel, after being irradiated with different laser parameters. In addition, the Ca/P ratio of each sample was evaluated by weight percentage. For this test, an artificial demineralization solution was prepared and applied to teeth samples. Each sample was weighed by 4-digit electric balance (Sartorius Lab Instruments GmbH&Co.KG, Goettingen, Germany), after being thoroughly dried by compressed air.

The samples were coated with nail varnish as an acid resistance, except for approximately 1.5×1.5 mm window on the treated surface for the demineralization test purposes. The demineralization solution contains 0.0022 M of $CaCl_2$, 0.05 M acetic acid, 0.0022 M of NaH_2PO_4, and few grams of KOH for adjusting the PH to 4.5. The polished samples were immersed individually in this solution at 37 °C for 48 h, and then washed by tap water for 5 min, then by deionized water and left on air to dry. Finally, the nail varnish was removed and the samples were dried well for the weight measurement and EDS analysis. The same procedure was repeated, but this time after immersing the samples in a re-mineralization solution, an artificial saliva contains 1% albumin, 75% methylcellulose, 0.062% potassium chloride, 0.034% dipotassium hydrogen phosphate, 0.01% sodium fluoride, 0.0166% calcium chloride, 4.69% dextrose, and 0.2% methylparaben as a preservative. According to Morton and Smith [20], the pH of human saliva is usually in the range 6.2–8.0. The PH of the solution was determined by a PH meter (Inolab PH7110) and it was 6.88. The samples were kept individually in the artificial saliva for 48 h, washed with tap water for 1 min, washed with deionized water, and then left in the air to dry. Finally, the nail varnish was removed from the samples and dried well by compressed air for the weight measurement and EDS analysis.

Experimental design

Irradiated surface areas of 3×3 mm^2 were performed on carbon black–coated teeth surfaces to enhance laser absorption. Alternatively, each sample was immersed in black ink water

Table 3 Laser treatments of the tooth sample subgroups of group 3

Subgroup	Step 1 parameters	Step 2 parameters
A	Control	–
L	5 pulses-100 mJ Nd:YAG laser combined with nanosilver	–
M	500 mJ Nd:YAG laser combined with nanosilver	–
N	500 mJ Nd:YAG laser combined with carbon black	500 mJ Nd:YAG laser combined with nanosilver

Table 5 Vickers microhardness test results for group 2

Subgroup name	Laser energy	No. of pulses	Microhardness (VHN)
A	0	0	403 ± 55
G	100	2	462.6 ± 5.8
H	100	3	623 ± 67
I	100	4	816.6 ± 60
J	100	5	870 ± 62
K	100	6	1009.7 ± 273

solution at a level slightly higher than the sample surface, then irradiated by laser. Nd:YAG laser was also employed with colloidal nanosilver solution to treat enamel surfaces. The procedural chart of the study are presented in Fig. 1.

UV-visible spectrometer showed an absorption peak of the silver nanocolloidal solution at 400 nm with an average silver nanoparticle size of 51.69 nm. An SEM image showed 100 nm silver nanoparticle size, because of the particle aggregation. Forty-eight samples were divided into three main groups, then each group was divided into subgroups, each comprises 3 tooth samples. Group 1 comprises 6 subgroups (A, B, C, D, E, and F); each was treated with a single laser pulse but with different laser energy fluence (Table 1). Subgroups in group 2 (A, G, H, I, J, and K), were treated by the same laser energy fluence but with different number of laser pulses (Table 2). Finally, group 3, labeled as A, L, M, and N, was treated with combined Nd:YAG laser and silver nanoparticles (Table 3). The samples in group 3 were immersed in the colloidal silver nanoparticles solution during laser irradiation, in which case the carbon black was not used. Subgroup (A) in all groups is the untreated control group. Vickers microhardness test was performed to evaluate the surface hardness modifications presumably caused by laser irradiation. This test was facilitated by using Digital Micro Vickers hardness tester TH 715, 2008, China, equipped with a square-based diamond indenter and a high-resolution optical microscope with × 400 magnification. Indentations were made under a 500 g load for 15 s.

SPSS version 25 software was used for data analysis in which non-parametric ANOVA (Kruskal-Wallis test) was used to compare between all subgroups followed by Scheefy Significant Difference post hoc test, to determine the highest significance of subgroups. Alpha < 0.05 was set as significant.

Results

The microhardness results (Tables 4, 5, and 6) indicated an increase in teeth enamel microhardness with laser energy. Multiple Comparisons results in Table 5 shows a highly significant statistical difference between control and subgroup k; $p < 0.001$, subgroup G and K with $p = 0.001$, subgroup C and K with $p = 0.004$, subgroup L and K with $p = 0.013$, subgroup F with K with $p = 0.02$ (excluded). The hypothesis test summary is given in Table 7. The subgroup F that received 700 mJ of laser energy was excluded because of the cracks inflicted at this high laser energy.

In group 1, the increased enamel microhardness lowers the tooth abrasion degree and as a result, increases tooth resistance to decay [18].

Null hypothesis means there are no difference in the microhardness values between the groups, and this gives "reject" in Table 7. We considered a p value < 5% is significant. The results have shown differences (p values) between the groups, which means "reject" of the null hypothesis. Figure 2 demonstrates the Atomic Force Microscope analysis images for A (control), B (300 mJ), D (500 mJ), K (6 pulses of 100 mJ), L (5 pulses 100 mJ combined with nanosilver), and N (500 mJ followed by 500 mJ combined with nanosilver) subgroup surfaces which elucidate the surface topography. Other groups revealed irregular surface topography and a wide range of grain diameter sizes. The samples' surfaces of group 3, which were treated with colloidal silver nanoparticles, shared the same structure of connected chain-like grain, unlike the surface of the samples without silver nanoparticles. The sample's surface was converted into a functionalized one by merging adjacent enamel grains to form a continuous series of peaks.

The enamel surface roughness of the treated samples has increased with increased laser energy fluence due to laser-induced crystallographic changes. The diameter size of enamel grains was changing under different treatment conditions. Enamel grain size became smaller at 300, 400, and 500 mJ laser energy, but larger than the control at 600 mJ and 700 mJ. Also, the diameter size of enamel grains of group 2 became smaller than the control at 2 and 3 pulses of 100 mJ laser energy, but larger than the control at 4, 5, and 6 pulses of 100 mJ laser energy. The SEM image of the enamel surface of control group (A) had a smooth surface area with little depressions, but this picture has changed after laser treatment.

Table 6 Vickers microhardness test results for group 3

Subgroup name	Laser treatment	Microhardness (VHN)
A	0	403 ± 55
L	5 pulses-100 mJ Nd:YAG laser combined with nanosilver	560 ± 13.7
M	500 mJ Nd:YAG laser combined with nanosilver	580.8 ± 27
N	500 mJ Nd:YAG laser, followed by 500 mJ Nd:YAG laser combined with nanosilver	607.6 ± 16.3

Table 7 Microhardness statistical analysis of all groups

	Null hypothesis	Test	Sig.	Decision
1	The distribution of VAR00001 is the same across categories of microhardness	Independent Samples Kruskal-Wallis test	.001	Reject the null hypothesis

The treated enamel surfaces demonstrate some fused and ablated areas with some craters and deposits which increase with the laser fluence. Some voids were also formed on the surfaces at high laser fluence due to the vaporization of water and organic components (Fig. 3).

Figure 4 demonstrates the treated depth of the laser effect on the enamel surface. It is approximately 40 μm for the 400 mJ–treated sample. Figure 4 b and c represent the cross section of the treated and untreated parts of an enamel sample.

It shows significant changes in the treated enamel structure where the rods of the laser-treated part are overlapping, sharper, and more interconnected with each other. This explains the high microhardness and resistance of the treated tooth against demineralization. EDX analysis revealed changes in the concentrations of enamel components. Calcium and phosphorus existing in hydroxyapatite crystals are the main inorganic ingredients of the dental hard tissue [21]. The treated samples demonstrated significant increase in the calcium to

phosphorus ratio which refers to the re-distribution of mineral components during melting and re-solidification [22]. However, some samples in group 3 had Ca/P values close to or lower than the control samples' value (Table 8).

Discussion

A significant increase in teeth enamel microhardness with laser fluence was noticed compared to non-treated teeth. This is attributed to fast laser heating and quenching of a thin enamel layer below surface, and to the laser ablation–shockwave plasma pressure that pushes inside during laser illumination [23, 24]. In group 2, the samples were treated with fixed laser energy fluence but with a different number of laser pulses. It shows higher microhardness values than group 1, where the ultimate shock wave effect was reached by many smaller shock wave components added together

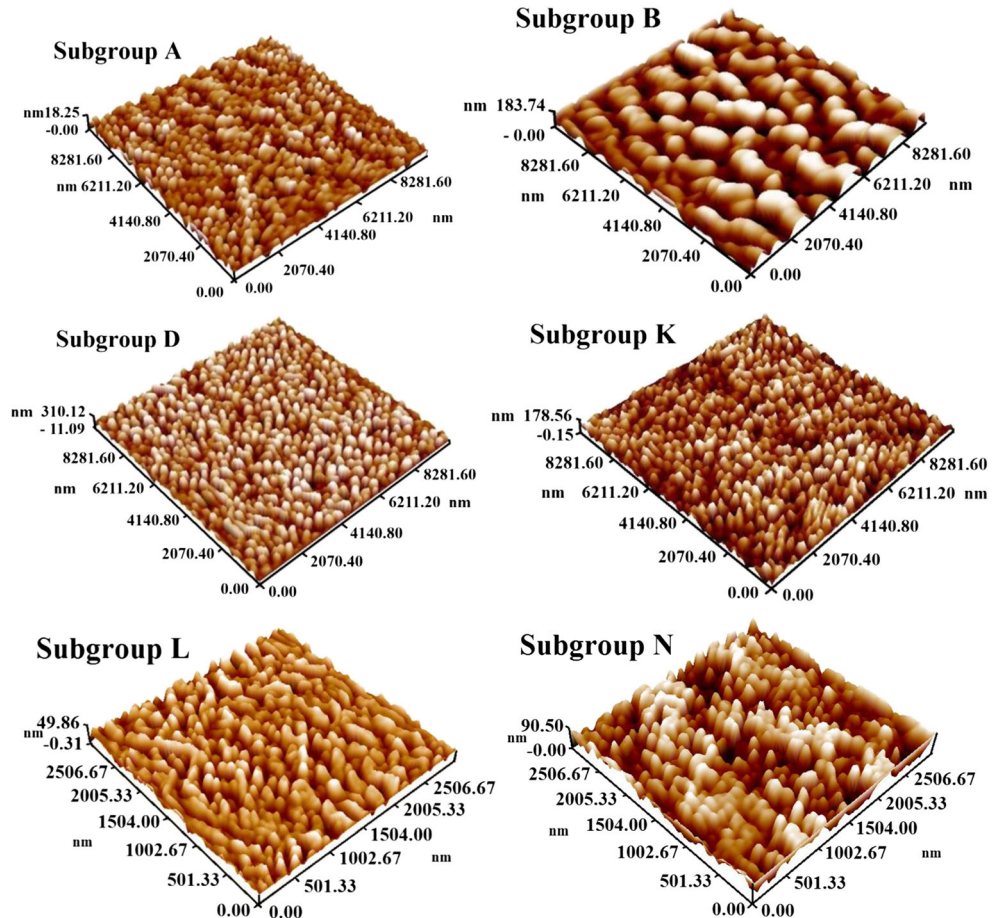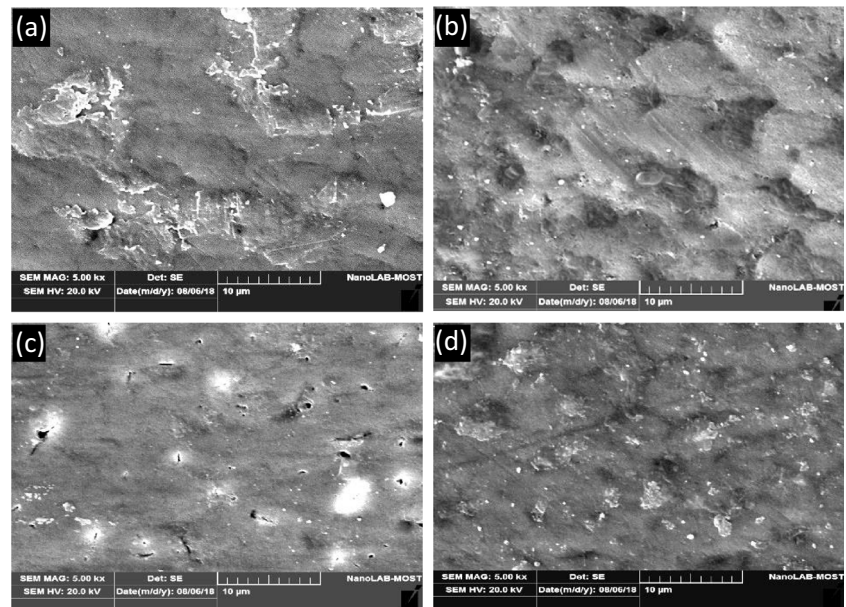**Fig. 2** 3D–AFM topographic images of some samples

Fig. 3 SEM images of enamel surface, **a** group A (control), **b** group B (treated with 300 mJ), **c** group D (treated with 500 mJ), and **d** group M (500 mJ laser combined with nanosilver)

without any probability of cracking. The greatest increase in microhardness was in subgroup K (600 mJ); however, this high microhardness value is not recommended as it could break the tooth at least pressure during mastication. Group 3 in which the samples were treated with combined silver nanoparticles and laser showed acceptable hardness values. Some samples in group 3 showed lower microhardness values despite the use of similar energy fluences, as for groups 1 and 2. This has resulted from using laser irradiation without covering the teeth samples with carbon black, i.e., losing large portion of the incident laser energy. Higher (not very high) tooth microhardness means higher tooth resistance against caries. This is because of the decrease in hydroxyapatite lattice stress and the reduction in enamel solubility after laser modifications of water, carbonate, and organic content of tooth mineral phases [25]. Figure 1 indicates a significant changes in the topography images between treated and control samples for the three main groups. The ideal granularity distributions and surface topography were in groups D (500 mJ), J (5 pulses of 100 mJ), and K (6 pulses of 100 mJ). The resulted increased roughness after laser treatment could be useful when treating teeth with adhesive restorative fluoride or silver nanoparticles as in

samples of group 3. Figure 5 shows the positive results of silver nanoparticles when combined with the laser irradiation. The figure indicates the role of silver nanoparticles in stabilizing the granules of the enamel surface tissue under the effect of laser irradiation. Group N (500 mJ, followed by 500 mJ combined with nanosilver) had the highest surface roughness value compared to other groups of group 3, because it had been treated with 500 mJ of Nd:YAG laser two times. Laser energy converted to heat in the dental hard tissue causes morphological, optical, and crystallographic changes in the dental enamel because of the chemical reaction resulting from heating enamel to high temperatures.

These morphologic changes may result from extending the organic matrix, phase transformation, and the blockage of ion diffusion pathways [22]. The thermal re-crystallization can increase the enamel crystal size and this makes the enamel more resistant to demineralization [26–28]. Enamel crystal size can change after laser treatment [29]. Between 200 and 400 °C, crystallites in enamel, at first, became smaller in size along the a-axis direction of the hexagonal phase, then grow bigger at temperatures beyond 400 °C [30]. This is fully consistent with the results of this study and the published results [6, 26–33] which
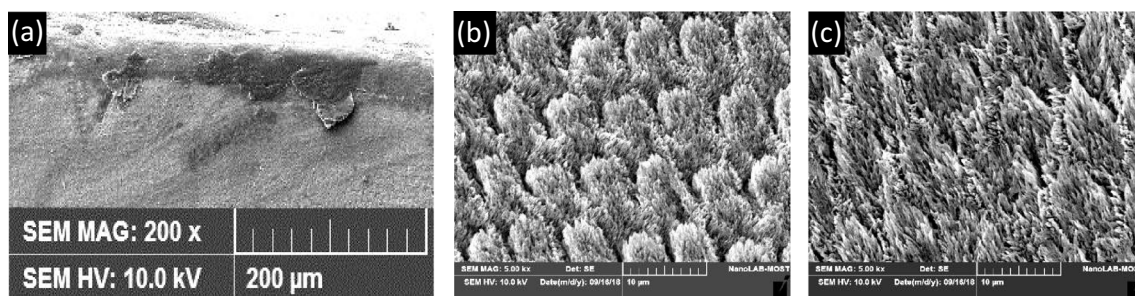

Fig. 4 **a** Longitudinal cross section of a 400 mJ–treated enamel sample (× 200), **b** the untreated enamel (× 5000), and **c** the treated enamel (× 5000)

Table 8   Ca/P weight ratios of group 3 before and after demineralization, and Ag percentage

Subgroup name	Ca/P ratio before and after demineralization		(Ag) weight percentage before demineralization
	Before	After 48 h	
A (control)	2.15	1.9	0.00
L (5 pulses 100 mJ combined with nanosilver)	2	1.976	0.17
M (500 mJ Nd:YAG combined with nanosilver)	1.986	2	0.26
N (500 mJ, followed by 500mJcombined with Nanosilver)	2.15	2.37	0.23

demonstrated a gradual growth in crystallites size along the c-axis. The water content is reduced when raising the temperature and a sudden reduction takes place at 250 to 300 °C leading to losing about one-third of the amount of water initially combined in enamel. At this same range of enamel temperature, water reduction concurs with a severe decrease of the lattice parameter (a-axis) [30, 34–36]. The a-axis length enlargement of the enamel crystallite is related to the structurally integrated water [37]. SEM images do not show observable changes in the heated enamel at temperatures below 300 °C, but enamel crystals are clearly demarcated and spotty micropores appear at 400 °C. These micropores increase in number and size at 500 °C, and an observable fusion is seen between adjacent enamel crystals [29]. Glass-like surfaces, cracks, and columns isolated by voids can be observed as the intensity of laser radiation increases [38]. When enamel is heated at a temperature around 200, inter-and intra-crystalline voids in the enamel can form. At 350 °C, the voids within the crystallites appear clearly. Between 350 and 600 °C, the size and number of voids increase significantly [39]. Every surface transformation comes from melting and following enamel re-crystallization during cooling. Low Ca/P values after laser treatment of some samples could be due to the coverage of calcium atoms by silver nanoparticles on the tooth surface. The weight percentages of the nanosilver particles on the treated teeth surfaces were acceptable in most samples.

The laser-treated enamel surfaces were immersed in the acid solution for 48 h to decrease the Ca/P ratio. The expected Ca/P decrease is caused by demineralization, since the extracted mineral leaves spaces on the surface which speed enamel demineralization with the existence of acid [22]. The demineralized samples of all laser-treated groups have higher Ca/P ratios compared to the demineralized control sample, indicating a low-rate demineralization of the laser-treated enamel surface. It is noteworthy pointing that after the demineralization test, there was no trace of silver nanoparticles on the surfaces of the tooth samples of group 3. This may explain the high Ca/P ratio after demineralization (Table 4). Mineral and chemical changes taking place in the enamel at high laser energy are responsible for the decrease in permeability and acid penetration within the internal layers [38]. Laser energy modifies the Ca/P mineral ratio and forms steadier and lesser acid soluble compositions, consequently lowering the chances for acids to attack the tooth and cause decay [40]. Whenever a change exists in the ratio between mineral and organic components, there is a change in the Ca/P ratio too. This could affect solubility, permeability, or adhesive specifications of the dental enamel [41]. It has been demonstrated that enamel mineral concentration reduction could increase porosity, leading to an increased caries' susceptibility and lower microhardness of dental enamel [42].

The relationship between enamel microhardness and mineral content, based on weight measurements, was demonstrated. The enamel microhardness increased with the increase of the Ca/P ratio, and this enhances tooth resistance to decay. The SEM images of the demineralized samples (Fig. 6) identifies deep voids on the surface of the demineralized enamel surface of group A (control), expressing a large amount of extracted minerals from the enamel surface. SEM images of other groups demonstrate lesser void depth, pointing out to a high concentration of minerals in the enamel surface and an increased acid resistance due to chemical (loss of organic matter and carbonate) [43], and physical (enamel fusion, melting, and re-crystallization) changes [7]. During these processes, the molten enamel may seal the ion channel in the dental hard tissue and delay the penetration of acid solution, therefore delaying minerals dissolution [22]. The SEM images of the demineralized samples demonstrate that the orientations of most enamel rods of the control sample were parallel to each other and perpendicular to tooth surface, while they became tangled with one another after laser treatment. This may decrease the acid penetration and increase the tooth resistance.
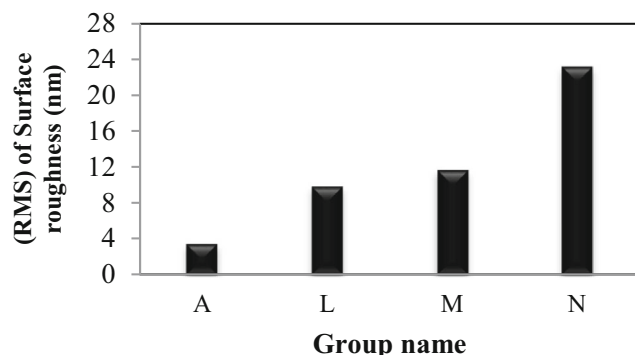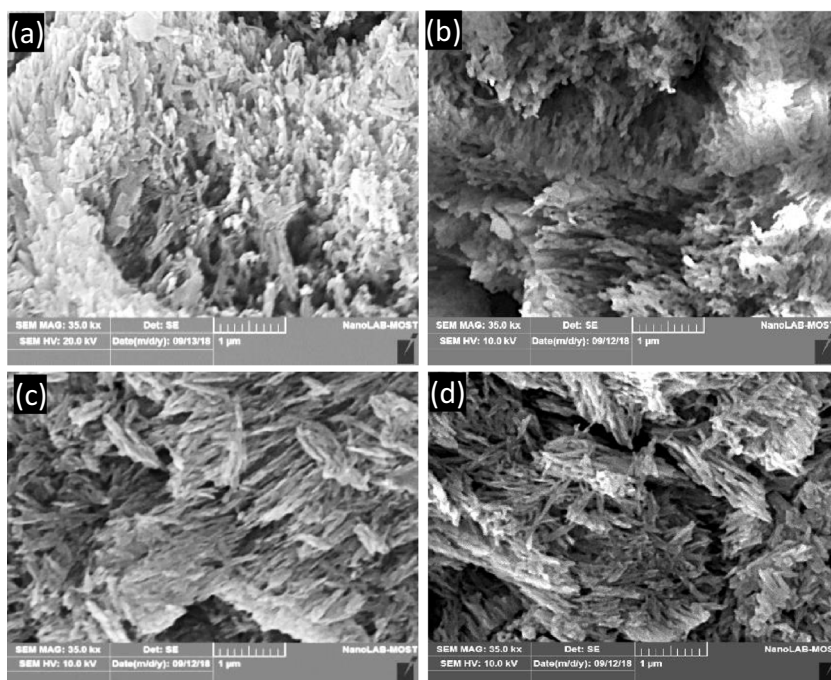

Fig. 5 Enamel surface roughness at different treatment conditions

Fig. 6 SEM image of the group samples after 48 h deminirelization: **a** subgroup A (control), **b** subgroup B (treated with 300 mJ laser), **c** subgroup J (treated with 5 pulses of 100 mJ laser), and **d** subgroup M (treated with 500 mJ Nd:YAG combined with nanosilver)

The weight measurement of samples after immersing one sample from each group in the demineralization solution for 48 h indicated a significant acid resistance improvement of the laser-treated enamel surface, i.e., reduced solubility, compared to control samples. For group 1, the highest acid resistance improvement ratio was 362% for subgroup D (500 mJ). For group 2, the highest acid resistance improvement ratio was 141.8% at 5 pulses of 100 mJ (subgroup J). For group 3, the highest acid resistance improvement ratio was 260% for subgroup N (500 mJ, followed by 500 mJ combined with nanosilver). The high value for subgroup N is consistent with the high microhardness value of the same group and has probably resulted from the use of carbon black during the laser illumination. Similar behavior of the three groups to the remineralization test was seen.

When dental enamel is treated with high laser energy fluence, some enamel modifications take place. These modifications begin when the protein starts to decompose at a temperature between 80 and 120 °C at the surface, until about 350 °C, with extreme oxidation and increased organic ingredients volatilization rate. The $[OH^-]$ content rises progressively between 300 and 500 °C [36]. The pyrophosphate $(P_2O_7^{4-})$ ions are formed by condensing the acid phosphate ions, and its content gradually increases between 200 and 400 °C. β-calcium pyrophosphate $(\beta\text{-}Ca_2P_2O_7)$ is formed at temperatures beyond 300 °C which is more resistant to acids [36, 47]. The above changes can influence ion diffusion and enamel dissolution during the acid attack. The minimal calcium dissolution takes place at 350 °C. It could be due to the pyrolysis products of the organic matrix, which closes up the newly formed porosity in the laser-heated enamel. The decrease of solubility at temperatures between 150 and 400 °C is the main factor for increasing acid resistance [35]. Between 400 and 460 °C [36], a glass-like phase is generated, and after 400 °C, the more soluble form of beta-tri-calcium phosphate (β-TCP) in the enamel is formed [39]. The extreme carbon content oxidation occurs at 500 °C [7]. At temperatures above 600 °C, carbonate hydroxyapatite is lost from the surface of the enamel apatite to the inner layers because of the laser heating effect. Enamel apatite melts at > 1000 °C, then β-TCP transforms to α-TCP at temperature > 1100 °C under ambient conditions, and tetra-calcium phosphate $Ca_4(PO_4)O$ can be formed at temperature > 1300 °C [27]. From above, the heat we can dump from the laser energy fluence used can decide the details of enamel surface modification. With all these chemical changes in the enamel structure, the enamel progressively loses its transportation materials (protein and water) and became more stabilized and more resistant against carries.

Conclusions

The laser illumination lowered the tooth abrasion degree and increased the tooth resistance to decay. The laser effect improved further after adding silver nanoparticles on the laser-modified enamel surface. The addition of silver nanoparticles improved the decay resistance by filling the ditches and microchannels found on the enamel surface with an antibacterial agent. Samples treated with laser and colloidal silver nanoparticles revealed connected chain-like grain, i.e., converting the surface into a functionalized one by merging the adjacent enamel grains to form a continuous series of spikes. The laser-treated depth of the enamel surface showed

overlapping sharp rods, interconnected with each other. This explains the high microhardness and acid resistance of the treated tooth against demineralization. The demineralized treated samples revealed higher Ca/P ratios compared to the demineralized control sample. The enamel acid resistance increased because the molten enamel seals the ion channel in the dentine and delay acid penetration. The decreased solubility after laser illumination is the main reason for increasing acid resistance. Our findings are in the context of previous work and are original in terms of establishing the relevant treatment protocol by using laser pulses and silver nanoparticles.

Compliance with ethical standards

Conflict of interest The authors declare that they have no conflict of interest.

Ethical approval The authors declare that all work presented in this paper was in accordance with the ethical standards of the institutional and/or national research committee and with the 1964 Helsinki declaration and its later amendments or comparable ethical standards.

References

1. Calif J, U.S. Department of Health and Human Services (2000). National Institute of Dental and Craniofacial Research, and National Institutes of Health. Dent Assoc (28): 685
2. Lima YB, Cury JA (2003) Seasonal variation of fluoride intake by children in a subtropical region. Caries Res 37(5):335–338
3. Wen X, Zhang L, Liu R, Deng M, Wang Y, Liu L, Nie X (2014) Effects of pulsed Nd:YAG laser on tensile bond strength and caries resistance of human enamel. Oper Dent 39(3):273–282
4. Florin R, Herrmann C, Bernhardt W (1990) Mikrohartemessungen a laser bearbeiteten Zahnoberflachen. Stomatol DDR 40:49–51
5. Attin T, Koidl U, Buchalla W, Schaller HG, Kielbassa AM, Hellwig E (1997) Correlation of microhardness and wear in differently eroded bovine dental enamel. Arch Oral Biol 42(3):243–250
6. Marquez F, Quintana E, Roca I, Salgado J (1993) Physical-mechanical effects of Nd:YAG laser on the surface of sound dental enamel. Biomaterials 14(4):313–316
7. Stern RH, Vahl J, Sognnaes RF (1972) Lased enamel: ultrastructural observations of pulsed carbon dioxide laser effects. J Dent Res 51(2):455–460
8. Anderson JR, Ellis RW, Blankenau RJ, Beiraghi SM, Westerman GH (2000) Caries resistance in enamel by laser irradiation and topical fluoride treatment. J Clin Laser Med Surg 18(1):33–36
9. Oho T, Morioka T (1990) A possible mechanism of acquired acid resistance of human dental enamel by laser irradiation. Caries Res 24(2):86–92
10. Mahori M, Manzon L, Pane S, Bedini R (2005) Effects of Nd:YAG laser on dental enamel. J Appl Biomater Biomech 3(2):128–133
11. Hibst R, Keller U (1989) Experimental studies of the application of the Er: YAG laser on dental hard substances: measurement of the ablation rate. Lasers Surg Med 9(4):338–344
12. Bahar A, Tagomori S (1994) The effect of normal pulsed Nd: YAG laser irradiation on pits and fissures in human teeth. Caries Res 28(6):460–467
13. Tagomori S, Morioka T (1989) Combined effects of laser and fluoride on acid resistance of human dental enamel. Caries Res 23(4):225–231
14. Huang GF, Lan WH, Guo MK, Chiang CP (2001) Synergistic effect of Nd:YAG laser combined with fluoride varnish on inhibition of caries formation in dental pits and fissures in vitro. J Form Med Assoc 100:181–185
15. Azevedo DT, Faraoni-Romano JJ, Derceli Jdos R, Palma-Dibb RG (2012) Effect of Nd:YAG laser combined with fluoride on the prevention of primary tooth enamel demineralization. Braz Dent J 23(2):104–109
16. Hiba IA, Ali SM (2015) The effect of Nd:YAG laser and casein-phosphor-peptide-amorphous calcium phosphate with fluoride on dental enamel de-mineralization: in vitro study, Iraqi dent. J 37(3):129–133
17. Morioka T, Suzuki K, Tagomori S (1984) Effect of beam absorptive mediators on acid resistance of surface enamel by Nd:YAG laser irradiation. J Dent Health 34:40
18. Valdeci ES Jr, Arnoldo VF et al (2014) A new silver-bullet to treat caries in children – nano silver fluoride: a randomised clinical trial. J Dent 42(8):945–951
19. Targino AG, Flores MA, dos Santos Junior V, de Godoy Bené Bezerra F, de Luna Freire H, Galembeck A, Rosenblatt A (2014) An innovative approach to treating dental decay in children. A new anti-caries agent. J Mater Sci Mater Med 25:2041–2047
20. Smith ME, Morton DG (2001) The digestive system. Elsevier health sciences
21. Erhan D, Meral AM, Nilgun OA, Firat O (2013) Effect of various laser irradiations on the mineral content of dentin. Eur J Dent 1:74–80
22. Kwon YH, Kwon OW, Kim HH (2003) Nd: YAG laser ablation and acid resistance of enamel. Dent Mater J 22:404–411
23. Montross C, Wei T, Ye L, Clark G, Mai Y (2002) Laser shock processing and its effects on microstructure and properties of metal alloys: a review. Int J Fatigue 10(10):1021–1036
24. Eisner K (1998) Process technological basis for the shock-hardening of metallic materials with a commercial excimer laser. Dissertation. University of Erlangen
25. Gary HW, Randall WE, Mark AL, Glen LP (2003) An in vitro study of enamel surface microhardness following argon laser irradiation and acidulated phosphate fluoride treatment. Pediatr Dent 25(5):497–500
26. Lin CP, Lee BS, Kok SH, Lan WH, Tseng YC, Lin FH (2000) Treatment of tooth fracture by medium energy CO_2 laser and DP-bioactive glass paste: thermal behavior and phase transformation of human tooth enamel and dentin after irradiation by CO_2 laser. J Mater Sci Mater Med 11:373–381
27. Rohanizadeh R, LeGeros RZ, Fan D, Jean A, Daculsi G (1999) Ultrastructural properties of laser irradiated and heat-treated dentin. J Dent Res 78(12):1829–1835
28. Ferreira JN, Palmera J, Phakey PP, Rachinger WA, Orams HJ (1989) Effects of continuous-wave CO_2 laser on the ultrastructure of human dental enamel. Arch Oral Biol 34(7):551–562
29. Sato K (1983) Relation between acid dissolution and histological alteration of heated tooth enamel. Caries Res 17(6):490–495
30. Sakae T (1988) X-ray diffraction and thermal studies of crystals from the outer and inner layers of human dental enamel. Arch Oral Biol 33(10):707–713
31. Young RA, Holcomb DW (1984) Role of acid phosphate in hydroxyapatite lattice expansion. Calcif Tissue Int 36(1):60–63
32. LeGeros RZ, Bonel G, Legros R (1978) Types of H_2O in human enamel and in precipitated apatites. Calcif Tissue Res 26(2):111–118
33. Askar CA, Moroz EM (1963) Pressure on evaporation of matter in a radiation beam. J Exp Theor Phys Lett 16:1638–1644

34. Corcia JT, Moody WE (1974) Thermal analysis of human dental enamel. J Dent Res 53(3):571–580

35. Hsu J, Fox JL, Higuchi WI, Otsuka M, Yu D, Powell GL (1994) Heat-treatment-induced reduction in the apparent solubility of human dental enamel. J Dent Res 73(12):1848–1853

36. Fowler BO, Kuroda S (1986) Changes in heated and in laser-irradiated human tooth enamel and their probable effects on solubility. Calcif Tissue Int 38(4):197–208

37. Holcomb DW, Young RA (1980) Thermal decomposition of human tooth enamel. Calcif Tissue Int 31(3):189–201

38. Tagomori S, Iwase T (1995) Ultra structural change of enamel exposed to a normal pulsed Nd:YAG laser. Caries Res 29(6):513–520

39. Palamara J, Phakey PP, Rachinger WA, Orams HJ (1987) The ultrastructure of human dental enamel heat-treated in the temperature range 200 degrees C to 600 degrees C. J Dent Res 66(12):1742–1747

40. Usumez S, Orhan M, Usumez A (2002) Laser etching of enamel for direct bonding with an Er,Cr:YSGG hydrokinetic laser system. Am J Orthod Dentofac Orthop 122(6):649–656

41. Ari H, Erdemir A (2005) Effects of endodontic irrigation solutions on mineral content of root canal dentin using ICP-AES technique. J Endod 31(3):187–189

42. Akkus A, Karasik D, Roperto R (2017) Correlation between microhardness and mineral content in healthy human enamel. J Clin Exp Dent 9(4):e569–e573

43. Borggreven JM, Van Dijk JW, Driessens FC (1980) Effect of laser irradiation on the permeability of bovine dental enamel. Arch Oral Biol 25(11–12):831–832